

Internal collision double ionization of molecules driven by co-rotating two-color circularly polarized laser pulses

Xue-Feng Li(李雪峰), Yue Qiao(乔月), Dan Wu(吴丹), Rui-Xian Yu(蔚瑞贤), Ji-Gen Chen(陈基根), Jun Wang(王俊), Fu-Ming Guo(郭福明), and Yu-Jun Yang(杨玉军)

Citation: Chin. Phys. B, 2024, 33 (**1**): 013302. DOI: 10.1088/1674-1056/acf5d8
Journal homepage: http://cpb.iphy.ac.cn; http://iopscience.iop.org/cpb

What follows is a list of articles you may be interested in

Generation of quasi-chirp-free isolated attosecond pulses from atoms under the action of orthogonal two-color combined pulse of fundamental frequency and higher intensity second harmonic fields

Rui-Xian Yu(蔚瑞贤), Yue Qiao(乔月), Ping Li(李萍), Jun Wang(王俊), Ji-Gen Chen(陈基根), Wei Feng(冯伟), Fu-Ming Guo(郭福明), and Yu-Jun Yang(杨玉军)
Chin. Phys. B, 2023, 32 (**6**): 063302. DOI: 10.1088/1674-1056/acc80a

Amplitude and rotation of the ellipticity of harmonicsfrom a linearly polarized laser field

Ping Li(李萍), Na Gao(高娜), Rui-Xian Yu(蔚瑞贤), Jun Wang(王俊), Su-Yu Li(李苏宇), Fu-Ming Guo(郭福明), and Yu-Jun Yang(杨玉军)
Chin. Phys. B, 2022, 31 (**10**): 103303. DOI: 10.1088/1674-1056/ac8ce8

Laser-induced fluorescence experimental spectroscopy and theoretical calculations of uranium monoxide

Xi-Lin Bai(白西林), Xue-Dong Zhang(张雪东), Fu-Qiang Zhang(张富强), and Timothy C Steimle
Chin. Phys. B, 2022, 31 (**5**): 053301. DOI: 10.1088/1674-1056/ac43a4

Study on the $A^2\Pi_{3/2u}$, $B^2\Delta_{3/2u}$, and $X^2\Pi_{3/2g}$ states of Cl_2^+ including its isotopologues

Wu Ling (吴玲), You Su-Ping (尤素萍), Shao Xu-Ping (邵旭萍), Chen Gang-Jin (陈钢进), Ding Ning (丁宁), Wang You-Mei (汪友梅), Yang Xiao-Hua (杨晓华)
Chin. Phys. B, 2015, 24 (**8**): 083301. DOI: 10.1088/1674-1056/24/8/083301

Ellipticity-dependent ionization/dissociation of carbon dioxide in strong laser fields

Zhang Jun-Feng (张军峰), Ma Ri (马日), Zuo Wan-Long (左万龙), Lv Hang (吕航), Huang Hong-Wei (黄红卫), Xu Hai-Feng (徐海峰), Jin Ming-Xing (金明星), Ding Da-Jun (丁大军)
Chin. Phys. B, 2015, 24 (**3**): 033302. DOI: 10.1088/1674-1056/24/3/033302

Internal collision double ionization of molecules driven by co-rotating two-color circularly polarized laser pulses

Xue-Feng Li(李雪峰)[1,2], Yue Qiao(乔月)[1,2], Dan Wu(吴丹)[3], Rui-Xian Yu(蔚瑞贤)[1,2], Ji-Gen Chen(陈基根)[4], Jun Wang(王俊)[1,2], Fu-Ming Guo(郭福明)[1,2], and Yu-Jun Yang(杨玉军)[1,2,†]

[1] *Institute of Atomic and Molecular Physics, Jilin University, Changchun* 130012, *China*
[2] *Jilin Provincial Key Laboratory of Applied Atomic and Molecular Spectroscopy (Jilin University), Changchun* 130012, *China*
[3] *School of Science, Jilin Institute of Chemical Technology, Jilin* 132022, *China*
[4] *Zhejiang Provincial Key Laboratory for Cutting Tools, Taizhou University, Jiaojiang* 318000, *China*

(Received 28 June 2023; revised manuscript received 13 August 2023; accepted manuscript online 1 September 2023)

The double ionization process of molecules driven by co-rotating two-color circularly polarized fields is investigated with a three-dimensional classical ensemble model. Numerical results indicate that a considerable part of the sequential double ionization (DI) events of molecules occur through internal collision double ionization (ICD), and the ICD recollision mechanism is significantly different from that in non-sequential double ionization (NSDI). By analyzing the results of internuclear distances $R = 5$ a.u. and 2 a.u., these two recollision mechanisms are studied in depth. It is found that the dynamic behaviors of the recollision mechanisms of NSDI and ICD are similar. For NSDI, the motion range of electrons after the ionization is relatively large, and the electrons will return to the core after a period of time. In the ICD process, electrons will rotate around the parent ion before ionization, and the distance of the electron motion is relatively small. After a period of time, the electrons will come back to the core and collide with another electron. Furthermore, the molecular internuclear distance has a significant effect on the electron dynamic behavior of the two ionization mechanisms. This study will help to understand the multi-electron ionization process of complex systems.

Keywords: non-sequential double ionization, internuclear distance, internal-collision, circularly polarized laser field

PACS: 33.20.Xx, 42.65.Ky **DOI:** 10.1088/1674-1056/acf5d8

1. Introduction

Interaction between intense laser fields (10^{13}–10^{16} W/cm^2) and atoms or molecules has led to many new physical phenomena, such as high-order harmonic generation (HHG),[1–8] above-threshold ionization (ATI),[9–13] non-sequential double ionization (NSDI)[14–16] and so on. The core physical process underlying these phenomena is the so-called recollision process:[17–19] One electron of the system is ionized and obtains energy in the laser field; as the direction of the laser electric field changes, the ionized electron has a certain probability of returning to the vicinity of the parent ion and re-colliding with it. This mechanism can produce double ionization (DI), and the curve of the divalent ion yield with the laser intensity shows a clear "knee" structure.[20] This ionization process is called NSDI.[21–23] In this process, the two electrons generated by the recollision process are highly correlated, which has attracted extensive attention from experimental[24,25] and theoretical researchers.[26,27]

With the deepening of research, the driving field used in the study of NSDI has gradually shifted from linearly polarized light to more complex light fields, such as counter-rotating and co-rotating two-color circularly polarized (TCCP) laser fields.[28–33] Strong high-order harmonic emission is observed by using the interaction between the counter-rotating TCCP field and the atom, and different order harmonics show circular polarization characteristics. The ellipticity of the harmonics is related to the order. Further research has been conducted on the photoelectron emission spectra and NSDI processes of atoms or molecules under the action of counter-rotating TCCP laser fields. For the co-rotating TCCP field, it is generally believed that the electrons cannot effectively go back to the nucleus, and the NSDI is significantly suppressed. However, Huang *et al*. theoretically investigated the NSDI of Ar in co-rotating TCCP laser fields with a three-dimensional classical ensemble model. Co-rotating TCCP fields can induce NSDI by the recollision process, while the yield is an order of magnitude lower than in the counter-rotating case. NSDI yield in co-rotating TCCP fields strongly depends on the peak field amplitude ratio of the two colors and achieves its maximum at a ratio of 2.4.[34] Therefore, it is proved that the chance of recollision between ionized electrons and parent ions can be affected by adjusting the electric field amplitude ratio of the co-rotating TCCP laser field.

Compared with atoms, molecules have additional vibrational coordinates (internuclear distance R), which makes the NSDI process more complicated. Tong *et al*. theoretically studied the internuclear distance dependence of the electron correlation in NSDI of H_2 using a strongly linearly polarized

†Corresponding author. E-mail: yangyj@jlu.edu.cn
© 2024 Chinese Physical Society and IOP Publishing Ltd

laser field. It was found that the correlated electron momentum spectra strongly depend on the internuclear distance R with a critical internuclear distance of about 4 a.u. for NSDI of H_2, where NSDI probability reaches a maximum.[35] These results provide insight into the important role of the structure of diatomic molecules in NSDI. Recently, Chen *et al*. checked the NSDI of molecules with different internuclear distances in the counter-rotating TCCP field.[36] The results are similar to those for the linear polarization field. In the counter-rotating TCCP field, with increasing internuclear distance, the NSDI yield of the molecule first increases and then decreases, reaching the maximum at $R = 4$ a.u. Through examining the ion momentum distribution under varied internuclear distances, it was discovered that the ion momentum distribution shows an inverted Y-shaped distribution at a small internuclear distance and a triangle-shaped distribution at a large internuclear distance. The results indicate that the dominant behavior of electron pairs evolves from correlation to anti-correlation with the increase of internuclear distance. In addition, the angle statistics of the final emission direction of the two electrons show that in the counter-rotating TCCP field, the two electrons from NSDI have a strong angular correlation.

Besides the study of the ionization process in the counter-rotating TCCP field, people have begun to investigate the ionization process of molecules under the effect of the co-rotating TCCP field. Wu *et al*. analyzed the DI process of hydrogen molecules with an internuclear distance of 2 a.u. under the action of co-rotating TCCP laser pulses, indicating that NSDI accounted for a vast weight in the DI yield. Regulating the peak field amplitude ratio of the co-rotating TCCP laser pulse can effectively adjust the trajectory of electrons so that the ionized electrons can recollide with the core producing NSDI.[37] Qiao *et al*. explored the HHG generation process of H_2^+ in the co-rotating TCCP field and the internuclear distance of the molecule strongly affects the harmonic intensity. With the increase of the molecular internuclear distance, the opportunity for recollision between ionized electrons and parent ions is enhanced.[38] However, there is still a lack of in-depth understanding of this process.

Thus, in this paper, with the classical ensemble model, we systematically study the DI process of hydrogen molecules driven by co-rotating TCCP laser fields. Our numerical results indicate that even when the SDI mechanism is dominant, the double ionization curve also exhibits an obvious "knee" structure. Through further analysis, it is found that this phenomenon originates from the fact that a considerable part of the DI events of molecules occurs through the internal collision double ionization (ICD) process. That is to say, in the co-rotating TCCP laser pulse, the energy obtained by the electron is not large enough to cause ionization, but the electron has the opportunity to be driven to a place relatively close to the nucleus, move around the nuclear area and then be driven back to the vicinity of the nucleus and collide with it. The two electrons are ionized in turn under the action of the laser field. During this collision process, the energy of the two electrons is always less than 0.

This paper is organized as follows. Section 2 presents the theoretical method of numerical calculations. The DI process of hydrogen molecules in the co-rotating TCCP field and the related physical mechanism are given in Section 3. The last section is a summary of our research work (atomic units are utilized throughout unless otherwise stated).

2. Theoretical model and numerical method

The method that we used in this paper is the classical ensemble method developed by Eberly, which has been widely used to describe strong-field double ionization processes qualitatively or quantitatively.[39–45] Although the molecule is essentially a quantum mechanical system, and the interaction between the molecule and the external laser field is described by the time-dependent Schrödinger equation of the multi-electron system, the computational load is very large.[46–48] The classical ensemble method provides a computationally efficient and physically intuitive approach to gain insights into strong-field double ionization problems, and its calculation results can better explain the observed experimental phenomena. Therefore, here we employ the classical ensemble method to study the ionization dynamics of H_2 by the TCCP laser field.

In this model, the evolution of the two-electron system is determined by Newton's equations of motion

$$\frac{\mathrm{d}^2 \boldsymbol{r}_i}{\mathrm{d}t^2} = -\nabla\left[V_{\mathrm{ne}}(\boldsymbol{r}_i) + V_{\mathrm{ee}}(\boldsymbol{r}_1, \boldsymbol{r}_2)\right] - \boldsymbol{E}(t), \tag{1}$$

where the subscript $i = 1, 2$ is the label of the two electrons, $\boldsymbol{r}_i$ is the coordinate of the electron and $\boldsymbol{E}(\mathrm{t}) = \boldsymbol{E}_\omega(t) + \boldsymbol{E}_{2\omega}(t)$ is the co-rotating TCCP laser field, where $\boldsymbol{E}_\omega(t)$ is the fundamental laser pulse and $\boldsymbol{E}_{2\omega}(t)$ is the second harmonic laser pulse. The laser pulses are written as

$$\begin{aligned}\boldsymbol{E}_\omega(t) = {} & \frac{E_0}{1+\gamma_E} f(t)\left[\cos(\omega t + \varphi_1)\,\hat{\boldsymbol{x}}\right. \\ & \left. + \sin(\omega t + \varphi_1)\,\hat{\boldsymbol{y}}\right], \end{aligned} \tag{2}$$

$$\begin{aligned}\boldsymbol{E}_{2\omega}(t) = {} & \frac{\gamma_E E_0}{1+\gamma_E} f(t)\left[\cos(2\omega t + \varphi_2)\,\hat{\boldsymbol{x}}\right. \\ & \left. + \sin(2\omega t + \varphi_2)\,\hat{\boldsymbol{y}}\right], \end{aligned} \tag{3}$$

where $\hat{\boldsymbol{x}}$ and $\hat{\boldsymbol{y}}$ are the unit vectors in the x and y directions, respectively. E_0 is the maximum amplitude of the combined laser field, γ_E is the amplitude ratio between the fundamental frequency laser pulse and the second harmonic one. Here, we set $\gamma_E = 3$. The frequency of the fundamental laser pulse $\omega = 0.0584$, and the corresponding wavelength is 780 nm. The second harmonic laser pulse $2\omega = 0.1168$, and the corresponding wavelength is 390 nm. The carrier-envelope phase

$\varphi_1 = \varphi_2 = 0$. $f(t)$ is a trapezoidal pulse envelope with two-cycle turn-on, six cycles at full strength, and two-cycle turn-off. The potentials of the ion–electron interaction and the electron–electron interaction can be given by

$$V_{\rm ne}(\boldsymbol{r}_i) = \frac{-1}{\sqrt{|\boldsymbol{r}_i - R/2|^2 + a^2}} + \frac{-1}{\sqrt{|\boldsymbol{r}_i + R/2|^2 + a^2}}, \quad (4)$$

$$V_{\rm ee}(\boldsymbol{r}_1, \boldsymbol{r}_2) = \frac{1}{\sqrt{|\boldsymbol{r}_1 - \boldsymbol{r}_2|^2 + b^2}}, \quad (5)$$

with the softening parameters $a = 1.5$ and $b = 0.05$ to avoid the autoionization and remove the numerical singularity, respectively.

In the calculation, we select H_2 as the target molecule, fix the hydrogen molecule nucleus on the x-axis, and study the double ionization at the internuclear distances $R = 2$ a.u. and 5 a.u. The ground state energies are -1.63 a.u. and -1.25 a.u., respectively. To obtain the initial conditions for Eq. (1), the ensemble is populated starting from a classically allowed position for the ground state energy of the target molecule. Given the position of two electrons, the kinetic energy of the two electrons is the difference between the ground state energy and the potential energy of the system. This available kinetic energy is randomly distributed between the two electrons. Then the electrons are allowed to evolve in the absence of the laser field to obtain stable position and momentum distributions. After the initial ensemble is obtained, a laser field is superimposed, and all electrons evolve in this laser field to obtain the corresponding trajectory. At the end of the laser field, DI, SDI, and NSDI yields of the ensemble are calculated based on the positions and momenta of two electrons. When the energies of both electrons are greater than 0 at the end of the laser field, we define it as a double ionization event that occurs. The single ionization time is defined as the instant of one electron achieving positive energy. After a period of single ionization, if the distance between the two electrons is less than 5 a.u. again, it is considered that a recollision occurs (the selection of recollision criteria does not affect the qualitative results). According to whether there exists a recollision during the double ionization process, the double ionization is further divided into NSDI and SDI.

3. Results and discussion

We first calculated the change of double ionization probability of hydrogen molecules with the laser intensity at two different internuclear distances, as shown in Fig. 1(a). It can be seen that the double ionization curves show a clear "knee" structure for both $R = 2$ a.u. and 5 a.u. Moreover, the double ionization yield is increased significantly at the internuclear distance of 5 a.u. compared with that at 2 a.u. In order to further explore the difference and connection of the double ionization mechanism under different internuclear distances, we systematically simulated SDI and NSDI yields in the double ionization yield of hydrogen molecules, then found the change of the parameter $S = (\mathrm{NSDI} - \mathrm{SDI})/(\mathrm{SDI} + \mathrm{NSDI})$ with the laser intensity, where NSDI and SDI correspond to the NSDI and SDI yields in the double ionization yield, respectively. From the definition of S, it can be observed that if the ionization mechanism is dominated by NSDI, S is positive, and if the ionization mechanism is dominated by SDI, S is negative. Therefore, the main mechanism of ionization can be judged by the S value. The calculated S values are shown in Fig. 1(b). It can be seen from the figure that for $R = 2$ a.u., the value of S gradually changes from positive to negative with the increase of the laser intensity, which means that the main mechanism of the hydrogen molecule double ionization is switched from the non-sequential ionization process to the sequential process. It should be noted that when $R = 5$ a.u., the main mechanism of the double ionization of hydrogen molecules is SDI with the increase of the laser intensity, but the double ionization curve also shows an obvious "knee" structure.

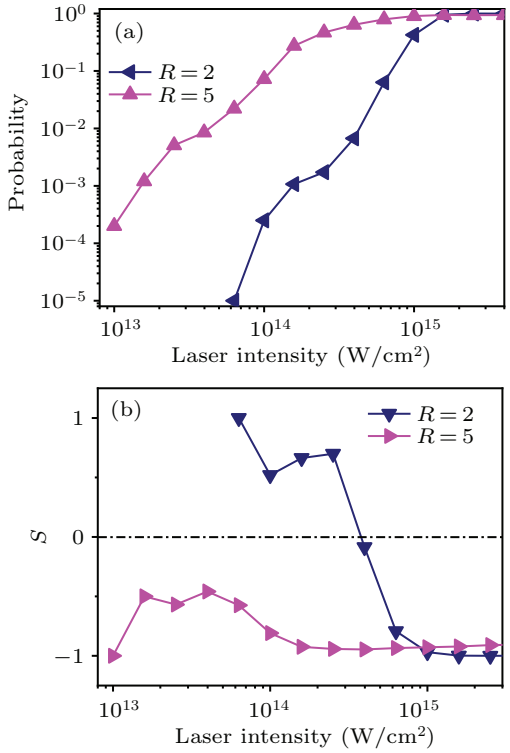


Fig. 1. (a) Double ionization yield as a function of the laser intensity; (b) double ionization asymmetry parameter as a function of the laser intensity.

To comprehend this unique feature, we tracked classical trajectories in the double ionization process at $R = 5$ a.u., as shown in Fig. 2. The double ionization mechanism includes not only NSDI but also ICD in the SDI process. In Fig. 2, we selected a laser intensity of 4×10^{13} W/cm^2 and traced NSDI, SDI, and ICD typical trajectories respectively. Figures 2(a), 2(c), and 2(e) display the function of the distance between the two electrons of NSDI, SDI, and ICD with time. Figures 2(b), 2(d), and 2(f) present the function of two electrons' energies

with time, which corresponds to Figs. 2(a), 2(c), and 2(e). For Figs. 2(a) and 2(b), it can be found from the trajectory information of the two electrons that an electron is first ionized by the laser field and driven away from the core, and then the ionized electron returns to the parent ion and collides with another electron. After the recollision process, the two electrons are ionized in turn, which is a typical NSDI recollision process. From Figs. 2(c) and 2(d), it can be seen that the two electrons are gradually driven away from the nuclear region and ionized in turn under the action of the laser field, and the two electrons have no correlation, which is a classical SDI process. Meanwhile, a discernible recollision phenomenon has been observed within the context of SDI, as depicted in Fig. 2(e). The difference from NSDI is that the electrons of SDI do not undergo the ionization process before the recollision occurs (as shown in Fig. 2(f), the energy is less than 0). The two electrons in the bound state always move around the nuclear region, but the electrons also have the opportunity to move relatively further away from the nucleus and move around the nuclear region and then collide with another electron. Notably, the energy exchange resulting from this recollision process remains modest, insufficient to induce electron ionization. Subsequent ionization of the two electrons is facilitated by the ensuing laser field. In this collision process, the energy of two electrons is always less than 0, prompting us to term this particular SDI process as internal collision double ionization (ICD). There are recollision processes after the single ionization time in NSDI, but not in SDI. If two electrons collide before the single ionization time in SDI and there is obvious energy transfer, it means that ICD exists in the double ionization process.

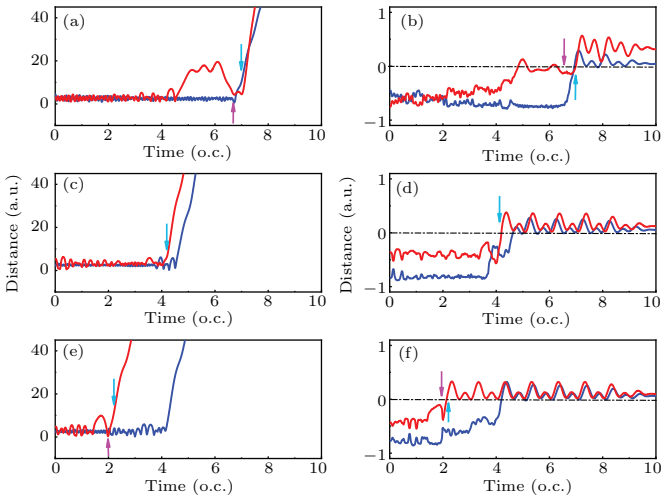


Fig. 2. Left column: The sample distance trajectories between the nucleus and each electron for different DI events. (a) NSDI mechanism of DI event; (c) SDI mechanism of DI event; (e) ICD mechanism of DI event. Right column: The sample energy trajectories of the two electrons, which correspond to the electron distance trajectories of the left column. The recollision time is marked by a pink arrow. The single ionization time is marked by a blue arrow.

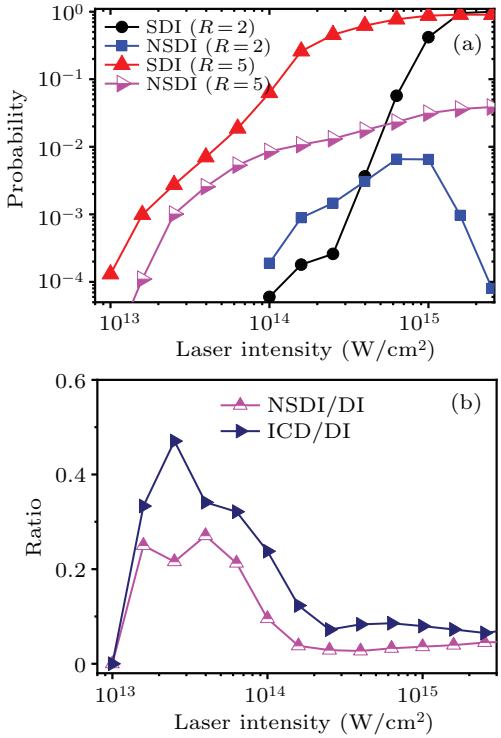


Fig. 3. In the case of $R=2$ a.u. and $R=5$ a.u., the yield of SDI and NSDI is a function of the laser intensity. (b) The ratio of NSDI yield and ICD yield to DI yield as a function of the laser intensity.

Through tracking the classical trajectory in the double ionization process, it is known that the double ionization mechanism includes the ICD process in addition to the generally considered NSDI process. In order to further explain why the double ionization mechanism with the large internuclear distance of 5 a.u. is dominated by SDI, and its double ionization curve also shows the obvious "knee" structure, we calculated the yield of NSDI and SDI under different internuclear distances as a function of the laser intensity, and the ratio of NSDI yield and ICD yield to the double ionization yield at $R=5$ a.u. as a function of the laser intensity. Figure 3(a) shows the SDI and NSDI yields as a function of the laser intensity in the case of $R=2$ a.u. and 5 a.u. It can be found that the non-sequential double ionization yield of hydrogen molecules is significantly enhanced in the case of the large internuclear distance of 5 a.u., indicating that the chance of recollision between the ionized electrons and the parent ions is increased, which is consistent with the results of Qiao *et al.*[38] Moreover, the sequential double ionization yield of molecules at a larger internuclear distance is also significantly enhanced, as due to the decrease of the molecular ionization energy with the increase of internuclear distance, it is easier for the electron to be ionized by the action of the laser field. Figure 3(b) exhibits the ratio of NSDI yield and ICD yield to the double ionization yield at $R=5$ a.u. as a function of the laser intensity. It can be observed that as the laser intensity increases, the ratio increases first and then decreases. The ICD yield in the double ionization mechanism is always higher than the NSDI yield.

With the increase of internuclear distance, the initial distribution range of hydrogen molecules is larger, and the probability of electron collision will increase, resulting in the ICD process being more likely to occur. This phenomenon shows that for the small internuclear distance of 2 a.u., the double ionization mechanism changes from NSDI to SDI with the increase of the laser intensity, which is similar to the case of the atom. The larger internuclear distance of 5 a.u. is always dominated by SDI, but the individual SDI still shows the "knee" structure characteristics, which are derived from the existence of the ICD process.

To clarify this process more clearly, we observed the potential difference between the NSDI and ICD mechanisms based on the ionization delay time of the recollision process. For each NSDI and ICD event, we recorded the single ionization time ($t_{\rm SI}$), the recollision time ($t_{\rm r}$), and the double ionization time ($t_{\rm DI}$). Here $t_{\rm SI}$ is defined as the time when the energy of the first electron (including kinetic energy, ion–electron potential energy, and half of the e–e potential energy) just becomes positive, and $t_{\rm DI}$ is defined as the time when both electrons obtain positive energy after the collision. For NSDI, $t_{\rm r}$ is defined as the time when the two electrons are closest after the first electron is ionized. For ICD, $t_{\rm r}$ is defined as the time when the two electrons are closest after the first electron is relatively far away from the nuclear region (the distance criterion is 2 a.u.). After analyzing all DI events, the statistics of these feature times can be obtained. In Fig. 4, we statistically analyzed the characteristic time of the DI event in the case of $R = 5$ a.u. Figure 4(a) shows the delay time in the process of the two recollision mechanisms, to put it another way, the difference between the single ionization time and the recollision time of the NSDI electron $(t_{\rm r} - t_{\rm SI})$, and the delay time between the ICD electron being far away from the nuclear region and the internal recollision moment $(t_{\rm r} - t_1)$. And t_1 is defined as when the electrons are in a higher excited state before the single ionization time (the distance between the two electrons is greater than 6 a.u., and the slight fluctuation of this criterion does not affect the final qualitative result). In the case of $R = 5$ a.u., the most likely value of $(t_{\rm r} - t_{\rm SI})$ reaches a peak at about 1.2 cycles, and the possible values are mainly distributed in 0–4 cycles. However, the most likely value of $(t_{\rm r} - t_1)$ reaches a peak at about 1.8 cycles, indicating that the recollision process of ICD has a longer delay time than that of NSDI. Figure 4(b) shows the difference between the recollision and the double ionization time $(t_{\rm DI} - t_{\rm r})$ of the NSDI and ICD processes. The results display that the $(t_{\rm DI} - t_{\rm r})$ of NSDI is mainly distributed in 0–2 cycles and peaks at 1.0 cycles, while the $(t_{\rm DI} - t_{\rm r})$ of ICD is mainly distributed in 0–6 cycles, and the most likely value reaches a peak at about 1.75 cycles. Therefore, compared with NSDI, ICD has a longer delay time between the double ionization and the recollision.

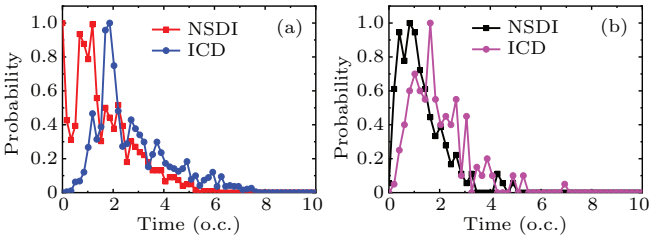


Fig. 4. (a) The delay time distribution between the single ionization and the recollision in the NSDI mechanism, and the delay time distribution between recollision and being far away from the nuclear region in the ICD mechanism. (b) The delay time distribution between the recollision and the double ionization of NSDI and ICD.

The above result indicates that when the internuclear distance is 5 a.u., the ICD process has a longer delay time than the recollision process of the NSDI process, and there is also a longer delay time between the double ionization and the recollision. Due to the larger internuclear distance of the molecule, the distribution of the two electrons is farther away from each other, which will lead to a large difference in the ionization and nucleus-return behavior of the electrons. In order to explore the influence of internuclear distance on the electron recollision behavior under various mechanisms, we selected the laser pulse with the peak intensity of 2×10^{14} W/cm^2 and analyzed the characteristic time of the DI event in the case of $R = 2$ a.u. Figure 5(a) gives the delay time in the process of the NSDI and ICD recollision mechanisms, namely, $(t_{\rm r} - t_{\rm SI})$ and $(t_{\rm r} - t_1)$. It can be observed that at $R = 2$ a.u., the most likely value of $(t_{\rm r} - t_{\rm SI})$ reaches a peak at about 0.27 cycles, and the possible values are mainly distributed in 0–2 cycles. Compared with the case of $R = 5$ a.u., there is a shorter delay time between the single ionization and the recollision. The most likely value of $(t_{\rm r} - t_1)$ reaches a peak at about 0.12 cycles, and the possible values are mainly distributed in 0–1 cycle, indicating that the re-collision process of the ICD process has a shorter delay time compared with the NSDI process. Compared with the ICD process in the case of $R = 5$ a.u., the delay time of the re-collision process is extremely short, indicating that the ICD electron returns to the nuclear region with a smaller internuclear distance. Since the initial distribution of electrons is close when the nuclear distance is small, it is easier for the electrons in the NSDI and ICD processes to return to the nuclear region in a shorter time after ionization. Figure 5(b) shows the difference between the recollision and the double ionization times $(t_{\rm DI} - t_{\rm r})$ of the NSDI and ICD processes. It is obvious that the $(t_{\rm DI} - t_{\rm r})$ of NSDI is mainly distributed in 0–6 cycles, and the peak appears at about 0.25 cycles. The peak value of $(t_{\rm DI} - t_{\rm r})$ of ICD appears in about 0.75 cycles, and the possible values are mainly distributed in 0–8 cycles. Compared with the NSDI process, the ICD process has a longer delay time between double ionization and recollision, which is consistent with the case of $R = 5$ a.u. It can be found that in the ICD mechanism, the delay time between the double ionization and the recollision is longer when $R = 2$ a.u. than when

$R = 5$ a.u. Because the second ionization energy is larger at a smaller internuclear distance, the ionization of the second electron mainly depends on the driving laser electric field, so $(t_{\rm DI} - t_{\rm r})$ is longer.

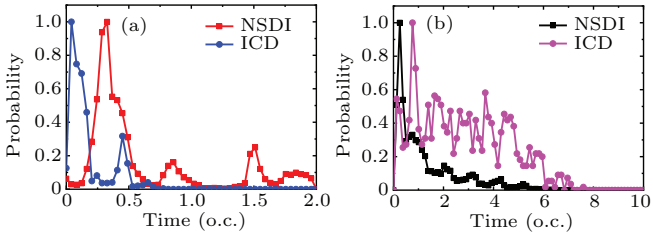


Fig. 5. Same as in Fig. 4 but the internuclear distance is 2 a.u.

The above analysis shows that different molecular nuclear distances have a great influence on the electron recollision in the ICD process. That is, when the nuclear distance is small, the ICD electrons are more likely to return to the nuclear region in a short time. To visually observe the potential dynamic behavior of NSDI and ICD mechanisms, we analyzed the motion behavior including the two electrons in two ionization mechanisms, as presented in Fig. 6. For $R = 5$ a.u., figures 6(a) and 6(b) are statistical distributions of the electronic position of the NSDI electron from the single ionization time to the recollision time and the ICD electron from the laser pulse start time to the single ionization time, respectively. For NSDI, the electron motion trajectory is different from that in the linearly polarized laser pulse. Under the action of the co-rotating TCCP laser, the motion behavior of electrons after the ionization is mainly rotated around the parent ion, and the motion range is far from the parent ion. After some time, it returns to the nucleus from a position far from the nuclear region. Compared with the recollision process of NSDI, the electron in the ICD process also rotates around the parent nucleus under the action of the light field before the ionization, but its motion range is relatively close to the nuclear area. After a while, the electron can return to the nucleus from the position near the nuclear area. Meanwhile, we calculate the results with $R = 2$ a.u., as presented in Figs. 6(c) and 6(d). It is also found that, for NSDI, the range of the motion of electrons after the ionization is far away from the parent ion, and after some time, it returns to the nucleus from a position far away from the nuclear region. The electron motion range of the ICD process is relatively close to the parent nucleus, and the electron will return to the nucleus from the position closer to the nuclear area. It is also found that, for NSDI, the dynamic behavior is similar either for $R = 5$ a.u. or $R = 2$ a.u. For the ICD mechanism, the range of electron motion is relatively small at the small internuclear distance of 2 a.u.

In the ICD mechanism of the co-rotating TCCP laser field, the two electrons in the bound state always move around the nuclear region before ionization occurs. The electrons will move to a higher excited state with the laser field, and then return to the parent ion to collide with it. Finally, under the action of the light field, the two electrons will be ionized in turn. The electron collision trajectory in the ICD process is different from the internal collision process driven by linearly polarized laser pulses.[49] In the linearly polarized field, the electronic movement is mainly limited to the one-dimensional space. After the electrons obtain energy, it is easy for them to move directly from one nucleus to another nucleus, collide with another electron, and then ionize successively. However, in the co-rotating TCCP laser field, the electrons are more inclined to the elliptical trajectory, and it is not easy for them to move directly from one nucleus to another nucleus for collision. Instead, after rotating motion to a higher excited state, the electron returns to the parent ion and collides with it. In essence, both collisions occur before the two electrons are deionized, but due to the polarization of the laser field, the trajectories of the collisions are significantly different.

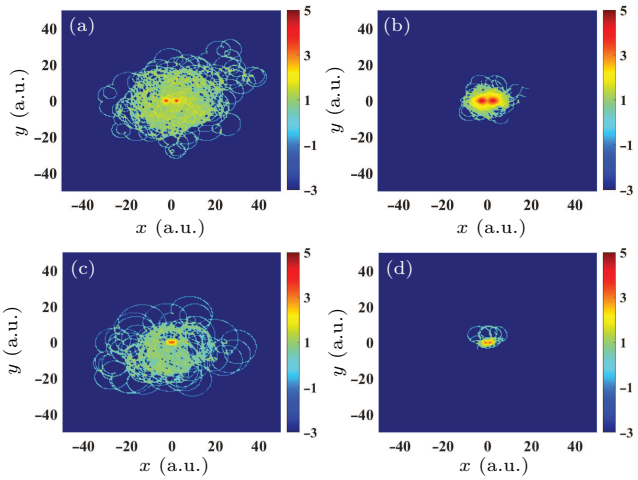


Fig. 6. The position distribution of NSDI electrons between the single ionization time and the recollision time (a) $R = 5$ a.u., (c) $R = 2$ a.u. The position distribution of ICD electrons before the single ionization time (b) $R = 5$ a.u., (d) $R = 2$ a.u.

4. Conclusions

In summary, we have theoretically studied the strong-field double ionization process of hydrogen molecules under the action of co-rotating TCCP laser pulses. We show that the double ionization curves reveal the same "knee" structural characteristics under the corresponding two different internuclear distances, but the double ionization mechanisms are significantly different. Analysis of its classical trajectory shows that the double ionization mechanism includes ICD in addition to the generally considered NSDI. Owing to the existence of the ICD process, the "knee" structure characteristics of the double ionization curve are obvious under the large internuclear distance. The analysis of the two ionization mechanisms of NSDI and ICD shows that the dynamic behaviors of the NSDI and ICD mechanisms with different internuclear distances are similar.

The NSDI electrons have a relatively large range of motion after the ionization. After some time, they return to the nucleus from a position far away from the nuclear region, while the ICD electrons have a relatively small range of motion, and the electrons will return from the position near the nuclear area after a while. In addition, the molecular internuclear distances have a great influence on the electron recollision behavior of the ICD process. That is, when the internuclear distance is small, ICD electrons are more likely to return to the nuclear region in a short time. Moreover, the ICD has a longer delay time between double ionization and recollision than the NSDI process under the two different internuclear distances. Therefore, the ionization time behavior of the ICD process can be regulated by changing the molecular internuclear distances. The ICD process contains rich dynamic information and has a significant impact on molecular double ionization yield, which is helpful for further understanding the strong field ionization mechanisms.

Acknowledgements

We acknowledge the National Key Research and Development Program of China (Grant No. 2019YFA0307700), the National Natural Science Foundation of China (Grant Nos. 12074145 and 11975012), Jilin Provincial Research Foundation for Basic Research, China (Grant No. 20220101003JC), and Jilin Provincial Education Department (Grant No. JJKH20230284KJ). The authors acknowledge the High Performance Computing Center of Jilin University for supercomputer time and the high performance computing cluster Tiger@IAMP.

References

[1] McPherson A, Gibson G, Jara H, Johann U, Luk T S, McIntyre I A, Boyer K and Rhodes C K 1987 *J. Opt. Soc. Am. B* **4** 595
[2] Ferray M, L'Huillier A, Li X F, Lompre L A, Mainfray G and Manus C 1988 *J. Phys. B: Atom. Mol. Opt. Phys.* **21** L31
[3] Krause J L, Schafer K J and Kulander K C 1992 *Phys. Rev. Lett.* **68** 3535
[4] Qiao Y, Huo Y Q, Jiang S C, Yang Y J and Chen J G 2022 *Opt. Express* **30** 9971
[5] Vampa G, Hammond T J, Thiré N, Schmidt B E, Légaré F, McDonald C R, Brabecand T and Corkum P B 2015 *Nature* **522** 462
[6] Qiao Y, Huo Y, Liang H, Chen J, Liu W, Yang Y and Jiang S 2023 *Phys. Rev. B* **107** 075201
[7] Zhao Y T, Xu X Q, Jiang S C, Zhao X, Chen J G and Yang Y J 2020 *Phys. Rev. A* **101** 033413
[8] Qiao Y, Chen J, Huo Y, Liang H, Yu R, Chen J, Liu W, Jiang S and Yang Y 2023 *Phys. Rev. A* **107** 023523
[9] Agostini P, Fabre F, Mainfray G, Petite G and Rahman N K 1979 *Phys. Rev. Lett.* **42** 1127
[10] Kruit P, Kimman J, Muller H G and van der Wiel M J 1983 *Phys. Rev. A* **28** 248
[11] Yuan H, Yang Y, Guo F, Wang J, Chen J, Feng W and Cui Z 2023 *Opt. Express* **31** 24213
[12] Paulus G G, Nicklich W, Xu H, Lambropoulos P and Walther H 1994 *Phys. Rev. Lett.* **72** 2851
[13] Yuan H, Yang Y, Guo F, Wang J and Cui Z 2022 *Opt. Express* **30** 19745
[14] Zhou Y, Huang C and Lu P 2011 *Phys. Rev. A* **84** 023405
[15] Ho P J 2005 *Phys. Rev. A* **72** 045401
[16] Zhou Y, Liao Q and Lu P 2009 *Phys. Rev. A* **80** 023412
[17] Corkum P B 1993 *Phys. Rev. Lett.* **71** 1994
[18] Yang B, Schafer K J, Walker B, Kulander K C, Agostini P and DiMauro L F 1993 *Phys. Rev. Lett.* **71** 3770
[19] Kamor A, Mauger F, Chandre C and Uzer T 2013 *Phys. Rev. Lett.* **110** 253002
[20] Walker B, Sheehy B, DiMauro L F, Agostini P, Schafer K J and Kulander K C 1994 *Phys. Rev. Lett.* **73** 1227
[21] Walker B, Mevel E, Yang B, Breger P, Chambaret J P, Antonetti A, DiMauro L F and Agostini P 1993 *Phys. Rev. A* **48** R894
[22] Larochelle S F J, Talebpour A and Chin S L 1998 *J. Phys. B: Atom. Mol. Opt. Phys.* **31** 1215
[23] Weber T, Weckenbrock M, Staudte A, Spielberger L, Jagutzki O, Mergel V, Afaneh F, Urbasch G, Vollmer M, Giessen H and Dörner R 2000 *J. Phys. B: Atom. Mol. Opt. Phys.* **33** L12
[24] Bergues B, Kübel M, Johnson N G, Fischer B, Camus N, Betsch K J, Herrwerth O, Senftleben A, Sayler A M, Rathje T, Pfeifer T, Ben-Itzhak I, Jones R R, Paulus G G, Krausz F, Moshammer R, Ullrich J and Kling M F 2012 *Nat. Commun.* **3** 813
[25] Wang Y, Xu S, Quan W, Gong C, Lai X, Hu S, Liu M, Chen J and Liu X 2016 *Phys. Rev. A* **94** 053412
[26] Ma X, Zhou Y and Lu P 2016 *Phys. Rev. A* **93** 013425
[27] Huang C, Zhong M and Wu Z 2018 *Opt. Express* **26** 26045
[28] Wu D, Li Q, Wang J, Guo F, Chen J and Yang Y 2021 *Chem. Phys. Lett.* **764** 138214
[29] Eckart S, Kunitski M, Ivanov I, Richter M, Fehre K, Hartung A, Rist J, Henrichs K, Trabert D, Schlott N, Schmidt L P H, Jahnke T, Schöffler M S, Kheifets A and Dörner R 2018 *Phys. Rev. A* **97** 041402
[30] Ke Q, Zhou Y, Tan J, He M, Liang J, Zhao Y, Li M and Lu P 2019 *Opt. Express* **27** 32193
[31] Han M, Ge P, Shao Y, Gong Q and Liu Y 2018 *Phys. Rev. Lett.* **120** 073202
[32] Chaloupka J L and Hickstein D D 2016 *Phys. Rev. Lett.* **116** 143005
[33] Ma X, Zhou Y, Chen Y, Li M, Li Y, Zhang Q and Lu P 2019 *Opt. Express* **27** 1825
[34] Huang C, Zhong M and Wu Z 2019 *Opt. Express* **27** 7616
[35] Tong A, Liao Q, Zhou Y and Lu P 2010 *Opt. Express* **18** 9064
[36] Chen Z, Su J, Zeng X, Huang X, Li Y and Huang C 2021 *Opt. Express* **29** 29576
[37] Wu D, Guo F M, Wang J, Chen J G and Yang Y J 2020 *Commun. Theor. Phys.* **72** 055503
[38] Qiao Y, Wu D, Chen J G, Wang J, Guo F M and Yang Y J 2019 *Phys. Rev. A* **100** 063428
[39] Panfili R, Haan S L and Eberly J H 2002 *Phys. Rev. Lett.* **89** 113001
[40] Ho P J, Panfili R, Haan S L and Eberly J H 2005 *Phys. Rev. Lett.* **94** 093002
[41] Haan S L, Breen L, Karim A and Eberly J H 2006 *Phys. Rev. Lett.* **97** 103008
[42] Haan S L, Van Dyke J S and Smith Z S 2008 *Phys. Rev. Lett.* **101** 113001
[43] Zhou Y, Liao Q and Lu P 2010 *Phys. Rev. A* **82** 053402
[44] Zhou Y, Huang C, Liao Q and Lu P 2012 *Phys. Rev. Lett.* **109** 053004
[45] Wang X, Tian J and Eberly J H 2013 *Phys. Rev. Lett.* **110** 073001
[46] Parker J S, Moore L R, Dundas D and Taylor K T 2000 *J. Phys. B: Atom. Mol. Opt. Phys.* **33** L691
[47] Panfili R, Eberly J H and Haan S L 2001 *Opt. Express* **8** 431
[48] Hu S X 2013 *Phys. Rev. Lett.* **111** 123003
[49] Tong A, Li Q, Ma X, Zhou Y and Lu P 2019 *Opt. Express* **27** 6415